



## Synthesis, Cytotoxicity, Molecular Docking and Molecular Modelling

### Studies of Complexes involving O, N-Donor ligands



CrossMark

Islam M. E. Moustafa<sup>1</sup>; Sahar M. Ibrahim<sup>1</sup>; Fatma M. A. El-Feky<sup>1</sup> and Mona A. Y. El-Etre<sup>2\*</sup>

<sup>1</sup> Chemistry Department, Faculty of Science, Benha University, Benha, Egypt

<sup>2\*</sup> Basic Science Department, Faculty of Engineering, Benha University, Benha, Egypt

\*Corresponding author; email: [monaeletr@yahoo.com](mailto:monaeletr@yahoo.com)

#### Abstract

For the development of novel antimicrobial and anticancer agents, complexation process between four azo dye ligands (AF1 – AF4) and Mn (II), Fe(III), Co(II) and Cu(II) ions were studied both in solution and in solid state. In solution, the stoichiometry of the formed complexes, studied by conductometric technique, was found to be (1:1), (1:2) and (2:1) (M:L). The proton – reagent stability constants of the free ligands and the metal – reagent formation constants of the formed complexes were determined by potentiometric titration technique. The greater values of the latter reflect the high stability of the complexes. The prepared solid complexes were characterized by elemental analysis, electronic spectra, FTIR, TGA and magnetic susceptibility measurement. Based on spectral data, different electronic d – d transitions within the complexes were assigned in terms of Tanabe - Sugano diagrams where octahedral geometry was deduced for all of them. The antimicrobial activity showed that selected compounds exhibit high activity against *Escherichia coli*, *Staphylococcus aureus* and *Candida glabrata*. These studies are supported by docking theoretical calculations to examine the binding interaction between the ligand AF2 and its complexes with the active site of DNA (HIV-1 reverse transcriptase (RT) in complex with TMC278). The cytotoxic activities of some selected metal complexes were tested against HEPG2 cell line. The relation between surviving cells and concentration of testing complexes is plotted to get the survival curve of each tumor cell line. The studied complexes seem to be promising as anticancer agents with IC<sub>50</sub> values ranged from 41 – 71 µg/ml. A group of measurements involving DMOL<sup>3</sup> program in materials studio package shaped for the recognized of wide scale Density Function Theory (DFT) were applied. From this study, the quantum chemical parameters and some energetic properties of ligand AF1 and its complexes were determined.

**Keywords:** azo compounds, metal complexes, Cytotoxicity, Molecular Docking, Molecular Modelling.

#### 1. Introduction

Azo dyes are important class of organic compounds which possess unique numerous properties in various fields such as dying in textile fibres plastics, leather, metal foil food, cosmetics, biological and clinical investigations and even the organic synthesis [1-3]. They have the ability to be used as drug carriers, either by acting as a 'cargo' that entrap therapeutic agents or by pro-drug approach. Besides drug-like and drug carrier properties, a number of azo dyes are used in cellular staining to visualize cellular

components and metabolic processes [4]. However, the biological significance of azo compounds, especially in cancer chemotherapy, is still in its infancy. This may be linked to early findings that declared azo compounds as one of the possible causes of cancer and mutagenesis. Currently, researchers are screening the aromatic azo compounds for their potential biomedical use, including cancer diagnosis and therapy [5-7]. Transition metals play an important role in preparing the bioactive compounds, which can interact with DNA by non-covalent interactions [8, 9]. The non-covalent way include three recognized binding modes of the tiny molecule to DNA are electrostatic interactions, groove binding

and external electrostatic binding. Among these, the intercalation mode of binding is very significant and coherent to the pharmacological activity of metal complexes [10]. In the present work, we present the preparation and characterization of four azo dye ligands (AF1 – AF4) based on 4-hydroxycoumarin and their Mn(II), Fe(III), Co(II) and Cu (II) complexes. The antimicrobial activity against *Escherichia coli*, *Staphylococcus aureus* and *Candida glabrata* was studied and supported by docking theoretical calculations. The cytotoxic activities of some selected metal complexes were tested against HEPG2 cell line and the IC<sub>50</sub> values were evaluated. The quantum chemical parameters and some energetic properties of the ligand AF1 and its complexes were determined by group of measurements involving DMOL<sup>3</sup> program in materials studio package shaped for the recognized of wide scale Density Function Theory (DFT).

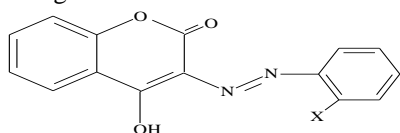
## Experimental

### Materials

All reagents used in the present study were of the highest quality (Merck, Aldrich, Fluka or Sigma Research Laboratories) and were used without further purification. 4-Hydroxycoumarin, o-aminophenol, aniline, o- anthranilic acid and o- chloroaniline were of purity 98% and were used without further purification. Freshly bidistilled water was used whenever water is necessary.

### Preparation of the azo compounds

The novel azo compounds were prepared by the usual way by coupling of 4-Hydroxycoumarin with diazonium salts of o- derivatives of aniline. They have the following structural formulae:



X = H (AF1), OH (AF2), COOH (AF3), Cl (AF4)

### Preparation of the solid complexes

Aqueous solutions of 1.00 mmol of metal chlorides were added dropwise with constant stirring to hot ethanolic solution of 1.00 mmol of each of the azo compounds and the mixture was refluxed for  $\approx$  6 hours. The mixture was left overnight whereby the solid complexes were precipitated. After cooling, the solid complexes were filtered off and washed with distilled water followed by ethanol and dried under vacuum.

### Studies on metal complexes in solution

### Conductometric titration

The measurements were carried out by titrating 50 mL of ligand solution ( $10^{-3}$  M) with the metal ion solution ( $10^{-2}$  M) as a titrant added from micro burette with mechanical stirring. The conductance of the resulting solution was then measured using YSI Model 32 conductance meter.

### Potentiometric titration

The following solutions were prepared:

(A): 5.0 mL of 0.1 M HCl and 5.0 mL of 1.0 M NaCl  
(B): Mixture (A) + 25 mL of  $10^{-3}$  M ligand (in ethanol)

(C): Mixture (B) + 2.0 mL of  $2.5 \times 10^{-3}$  M metal ion solution

Each solution mixture was completed to 50.0 mL using ethanol and bi- distilled water so as to obtain 70% by volume ethanol. Each mixture was then titrated against 0.02 M NaOH solution containing the same percent of ethanol running from an automatic micro burette with constant stirring.

### Physical measurements

Elemental analysis, Fourier-transform infrared spectroscopy (FTIR), thermal analysis, electronic spectra, magnetic susceptibility and molar conductivity measurements were all as mentioned in our previously work [11].

### Antimicrobial Screening

The antimicrobial activity of some solid complexes is tested against *Escherichia coli* (*E. coli*) as Gram-negative, *Staphylococcus aureus* (*S. aureus*) as a Gram-positive and *Candida glabrata* (*C. glabrata*) by the disk diffusion technique developed by Bauer *et al.* [12]. Three replicas were made for each treatment to minimize error.

### Antitumor activity assay

The cytotoxic activity of some selected metal complexes was tested against HEPG2 cell line and compared to that of Vinblastine as a standard drug. The relation between surviving cells and tested concentration was plotted to get the survival curve of each tumor cell line. The 50% inhibitory concentration (IC<sub>50</sub>) was estimated from graphic plots of the dose response curve for each concentration [13, 14]. All measurements were carried out at the Regional Centre for Mycology and Biotechnology, Al-Azhar University, Cairo, Egypt.

### Molecular docking

The antimicrobial activity studies are supported by computational methods such as molecular docking. All of the molecular studies were carried out on an Intel core i7, 16 GB memory, with a Windows 10 operating system, using Molecular Operating Environment (MOE 2015.10; Chemical Computing

Group, Montreal, Canada) as the computational software [15].

### Molecular modelling

The cluster calculations using DMOL<sup>3</sup> program [16] in materials studio package [17] which is designed for the realization of large scale density functional theory calculation (DFT) were performed. DFT semi-core pseudopotentials calculations (dspp) were performed with the double numerical basis sets plus polarization functional (DNP). The DNP basis sets are of comparable quality to 6-31 G Gaussian basis sets [18].

## Results and discussion

### 1- Studies on the metal complexes in solutions

In this part the possibility of complex formation between ligands and metal ions in solution is discussed. The stoichiometry of the complexes formed was studied by conductometric titration while the proton – ligand stability constants of the free ligand and the metal – ligand formation constants of the complexes was determined by potentiometric titration.

#### 1-1 Conductometric titration

The stoichiometry of the complexes formed between Mn<sup>2+</sup>, Fe<sup>3+</sup>, Co<sup>2+</sup>, and Cu<sup>2+</sup> and the azo compounds under study is studied by conductance measurements method which provide information about the type of complexes formed and the mode of interaction of the ligand with the metal ion. The solution used as a titrant should be relatively more concentrated than that of the solution being titrated. The conductance measured (after correction for dilution by the factor  $[V_0 + V_I / V_I]$  where  $V_0$  is the original volume of the solution (50.0mL) and  $V_I$  is the volume of the titrant.) is then plotted as a function of the molar ratio (ligand / metal). In the present work, the common behavior of the conductance – molar ratio curves is the increase in conductance with the increase of the volume of the titrant (*c.f.* Fig. 1). They are represented by intersecting straight lines the slope of which showed significant changes when the mole ratio ( $C_L:C_M$ ) was about 2:1, 1:1 and 1:2; thus indicating the formation of a relatively stable 2:1, 1:1 and 1:2 complexes (M:L) between M<sup>n+</sup> and ligands. The increase in conductance cannot be attributed only to the liberation of H<sup>+</sup> during metal ion – ligand interaction, but it can be also explained by the fact that the metal ion in ethanol medium form coordination bonds with the chloride ions, that would exhibit an apparent covalent nature (Cl-M-Cl)[19]. On complex formation, the chloride ions are preferentially expelled and migrate relatively free leading to an increase in conductance.

#### 1-2 Potentiometric Alkalimetric Titration

Potentiometric method is one of the most accurate and widely used techniques currently available for the study of ionic equilibrium and determination of stability constants of complexes formed in solution. The potentiometric titrations were performed in presence of acid mixture (A), mixture as medium consisting of 0.1 M HCl and 1.0 M NaCl, mixture (B) containing the azo compounds of concentration of  $1 \times 10^{-3}$  M and mixture (C<sub>n</sub>) containing different metal ions of concentration of  $2.5 \times 10^{-3}$  M as recommended by Bjerrum [20]. In all mixtures A, B or C<sub>n</sub>, absolute ethanol of 40% (v/v) is enough to keep the components of the mixture in soluble state. These mixtures were then titrated with 0.02 M NaOH freed from carbonate containing also 40% (v/v) ethanol to keep the ratio of ethanol in the titration vessel constant. The potentiometric titration curves are S – shaped with a sharp jump in mixtures (A) and (B) but relatively smooth curves are obtained with mixtures C<sub>n</sub> which contain the metal ions (*c.f.* Fig.2- a as an example). The end points for the titration of the mixtures increase in the order A < B < C<sub>n</sub>. The average number of protons associated with the ligand molecule; n'A at different pH values are determined using the equation

$$n'_{A=Y} = \frac{(V_1 - V_2)(N^0 + E^0)}{(V^0 + V_1)(TC_{Lo})}$$

Plotting of n'A against pH of the solution gives proton – ligand formation curves shown representatively in Fig.2-b. From these curves the proton – ligand stabilities of the ligands are calculated, and the data are cited in Table (1). The average number of ligand molecules attached per metal ions n' at different pH's are calculated with the free ligand exponent pL using the equations

$$n' = \frac{(V_2 - V_3)(N^0 + E^0)}{(V^0 + V_1) n'A(TC_{Mo})} \quad (5)$$

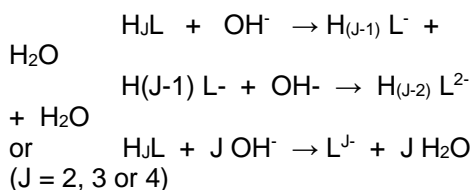
$$Pl = \log \frac{\sum_{n=0}^{n=j} \beta_n^H \left( \frac{1}{\text{antilog } pH} \right)^n}{(TC_{Lo} - n' TC_{Mo})} \times \frac{V^0 + V_3}{V_0} \quad (6)$$

Example of the metal – ligand formation curves (n' – pL) is shown in Fig.2-c from which the metal – ligand stability constants are calculated, and the data are cited in Tables (1). In the above equations, TC<sub>Mo</sub> the total concentration of metal ion present in solution, β<sub>n</sub>H the overall stability constant, V<sub>1</sub>, V<sub>2</sub> and V<sub>3</sub> are the volumes of

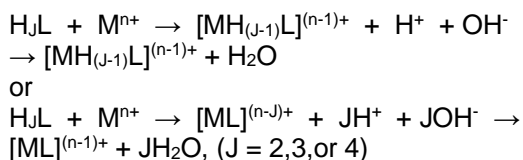
NaOH required to reach the same pH in titration curves in acid mixture, organic ligand and the complex respectively,  $V^0$  the initial volume (50 mL),  $TC_{L_0}$  the total concentration of the ligand,  $Y$  the total number of dissociable protons attached to the ligand,  $N_0$  the normality of NaOH solution and  $E^0$  the initial concentration of the free acid.

The mechanism of the reaction between the various ligands and metal ions during the addition of NaOH can be represented as:

a- In case of ligand mixture:



b- In case of metal – ligand mixture:



From titration results, recorded in Table (1), it is found that the values of the overall proton ionization constants increase when the hydroxyl group in *o*- position to the  $-N=N-$  linkage is replaced by a carboxylic group. Also, all the ligands under study form chelates with  $Mn^{2+}$ ,  $Fe^{3+}$ ,  $Co^{2+}$  and  $Cu^{2+}$  ions. Though, the stability of the chelates showed no regular behavior with the metal ions used, but it can be noticed, generally that the stability increases with the increase in both ionization potential and  $e/r$  ratio with little deviation.

The ligands under investigation have many active centres for chelate formation viz  $-N=N-$ ,  $C=O$ ,  $OH$  or  $COOH$  groups so, it can be thought that the interaction of metal ion takes place through covalent linkage between the metal ion and the oxygen atoms of hydroxylic or carboxylic groups in *o*- position to the azo centre in addition to coordinate bonds with the latter.

## 2- Studies on the metal complexes in solid state

### 2-1 Elemental analysis and Molar conductivity

The  $Mn^{2+}$ ,  $Fe^{3+}$ ,  $Co^{2+}$  and  $Cu^{2+}$  complexes formed by the reaction of metal chloride salts with azo compounds were studied and their chemical structure are discussed. All complexes

are coloured, stable in air and have high decomposition points. They are freely soluble in dimethylsulphoxide (DMSO) and dimethylformamide (DMF) but sparingly soluble in other common organic solvents. Results of elemental analysis of some selected complexes (Table 2) are in good agreement with the calculated values of the proposed formulae. The molar conductance ( $\Lambda_m$ );  $ohm^{-1}cm^2mol^{-1}$  of the studied complexes were measured in solutions of DMF. The values shown in Table (2) indicate the ionic nature of the complexes formed with number of ions equals two or three (in case of  $Fe^{3+}$  complexes). The presence of the anion ( $Cl^-$ ) outside the coordination sphere is confirmed by the precipitation of  $Cl^-$  as  $AgCl$  by the addition of  $AgNO_3$  solution to the solubilized chelates in DMF.

### 2-1 Thermal analysis

Inspection of the TG – DT curves shows that the complexes degrade thermally within the temperature range  $30^\circ C - 570^\circ C$  through three main steps:

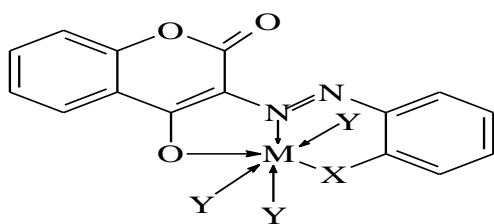
i- Dehydration of physically adsorbed and coordinated water molecules from the coordination sphere takes place within the temperature range  $50.0^\circ C - 177.40^\circ C$

ii- Starting decomposition of the unhydrated complexes through the second step within the range  $225.0^\circ C - 330^\circ C$  range leading to evolution of  $N_2$  and  $CO_2$  gases.

iii- Full thermal decomposition through the third step started at  $527.0^\circ C$  leading to the metal oxides as final products.

### 2-3 Infrared spectra

The IR spectral study showed that the free ligands exhibit strong band characteristic for the stretching vibrations of carbonyl ( $\nu_{C=O}$ ), hydroxyl ( $\nu_{OH}$ ) and azo ( $\nu_{N=N}$ ) groups. These bands suffer a notable shift to lower frequencies in the spectra of complex species as a result of donation of lone pairs of electrons to form the coordination bonds. The far infrared region of the spectra of the metal chelates shows two new bands due to the stretching vibrations of  $M-O$  and  $M-N$  bonds. Accordingly these ligands act as monobasic bidentate in ON fashion and the mode of bonding can be represented as follows:



M = Mn, Co, Fe, Cu

X = H (AF1) [HL], OH (AF2) [H2L], COOH (AF3) [H2L] and Cl (AF4) [HL]

2-4- Magnetic susceptibility and electronic absorption spectra

**Magnetic susceptibility** measurements at room temperature exhibit paramagnetism for Fe(III), Mn(II), Co(II) and Cu(II) complexes as expected from their electronic configuration. The room temperature values of the effective magnetic moment ( $\mu_{\text{eff}}$ ) for Mn(II) and Fe(III) complexes span the 5.14–6.05 BM interval, which are close to the theoretical spin-only value for  $S = 5/2$ , equal to 5.9 BM which support the high spin state of these complexes. High spin octahedral complexes of Co(II) have magnetic moments ranging from 4.77 to 5.22 B.M. They have large orbital contribution since the spin only formula for three unpaired electrons is only 3.88 B.M. This value is attributed to threefold orbital degeneracy  ${}^4T_{1g}$  ground state.[21]. The observed magnetic moments for the Cu(II) complexes are 1.77 and 1.90 BM suggesting a distorted octahedral geometry for Cu(II) complex[22].

**Electronic absorption spectra** of the complexes were studied in solid state (using Nujol mull technique) and compared to those of the free ligands. The spectral data are given in Table (3). which indicate that:

1- For Mn(II) and other  $d^5$  cases, the ground state is  ${}^6S$  and higher states include,  ${}^4G$ ,  ${}^4D$ ,  ${}^4P$   ${}^4F$  etc. It is expected that since there are NO spin-allowed transitions possible, the electronic spectrum should only contain very weak bands. The electronic spectra of Fe(III) – AF2 complex display three bands at 91138.1, 22780.8 and 10161.8  $\text{cm}^{-1}$  assignable to  ${}^6A_{1g}(S) \rightarrow {}^4T_{1g}(G)$ ,  ${}^6A_{1g}(S) \rightarrow {}^4T_{2g}(G)$  and  ${}^6A_{1g}(S) \rightarrow {}^4E_g, {}^4A_{1g}(G)$  transitions, respectively, indicating that the complex possesses a high spin octahedral configuration [23].

2- The electronic spectra of the octahedral Co(II) complexes exhibit absorption bands assigned to  ${}^4T_{1g}(F) \rightarrow {}^4T_{2g}(F)$  ( $\nu_1$ ),  ${}^4T_{1g} \rightarrow {}^4A_{2g}$  ( $\nu_2$ ), and  ${}^4T_{1g}(F) \rightarrow {}^4T_{1g}(P)$  ( $\nu_3$ ) transitions in the NIR–VIS region ( $\nu_1$ : 8811–11,635  $\text{cm}^{-1}$ ;  $\nu_2$ :

13,550–16,447  $\text{cm}^{-1}$ ;  $\nu_3$ : 18,553–19,260  $\text{cm}^{-1}$ ) [24].

3- Copper (II) complexes show two spin allowed transition bands at 30303  $\text{cm}^{-1}$  and 33333.3  $\text{cm}^{-1}$  due to the  ${}^2a_{1g}(D) \rightarrow {}^2b_{1g}(D)$  and  ${}^2e_g(D) \rightarrow {}^2b_{1g}(D)$  transitions, respectively. It was reported that Cu (II) complexes showed a broad asymmetric band in the region 20576  $\text{cm}^{-1}$  expected for a d-d transition of an octahedral Cu(II) complex [25]. The broadness of the band could be attributed to the overlapping of several bands as a result of strong Jahn-Teller distortion expected in a  $d^9$  ion [26].

## 2-5 Antimicrobial activity

The antimicrobial activity of some solid complexes is tested against *Escherichia coli* (*E. coli*) as a Gram-negative, *Staphylococcus aureus* (*S. aureus*) as a Gram-positive and *Candida glabrata* (*C. glabrata*). The antibacterial results (*c.f.* Table 4) showed that the selected studied complexes exhibit high activity against the tested organisms compared to levofloxacin taken as a standard drug.

Results of antibacterial activity reveal that the ligands under study and their complexes were found to be potentially active against *E.coli* and moderately active against *S. aureus* and *C. glabrata*. This simply, due to inhibitory activity of ligands related to the cell wall structure of the bacteria. In general, the membrane of gram-negative bacteria was surrounded by an outer membrane containing lipopolysaccharides. The ligands appear to be able to combine with the lipophilic layer to increase the membrane permeability of the gram-negative bacteria. Therefore, the lipophilicity plays a significant role in causing the death of the gram-negative bacteria [27]. Moreover, the synergistic effect of metal complexes enhances the antimicrobial activity; this may be explained by chelation theory.

On chelation the positive charge of metal is partially shared with the donor atoms present in the ligands; there may be  $\pi$ -electron delocalization over the whole chelating. This increases the lipophilic character of the metal chelate and favours its penetration through the lipid layer of the bacterial membranes. Chelation is not only the criterion for antibacterial activity; it is expected to be a function of steric, electronic, and pharmacokinetic factors along with mechanistic pathway. Other factors such as

solubility, conductivity, dipole moment, size of metal ions, stability constants of the complexes, and their magnetic moments are also reported to affect the microbial activity of the complexes [28]. This enhancement in the activity is also rationalized due to presence of azo (N=N) group. In addition, the formation of hydrogen bonds through the functional groups with the active centers of various cellular constituents, resulting in interference with normal cellular processes [29]. Furthermore, the ligands with nitrogen and oxygen donor systems might inhibit enzyme production, since the enzymes which require these groups for their activity appear to be especially more susceptible to deactivation by the metal ions upon chelation [30].

### 2-6 Antitumor activity

The cytotoxic activities of some selected metal complexes were tested against HEPG2 cell line and compared to that of Vinblastine as a standard drug. The 50% inhibitory concentration (IC<sub>50</sub>) was estimated from graphic plots of the dose response curve for each concentration. Inspection of the cytotoxic data, it is found that the efficiency of the complexes are arranged as AF2 – Cu(II) > AF1 – Fe(III) = AF2 – Co(II). The enhanced activity of metal complexes may be attributed to the increase in conjugation in the ligand moiety takes place in complexation process.

Shier [31] suggested that compounds having IC<sub>50</sub> values 10 – 25 µg/ml are considered to have weak cytotoxic activities, while those having values ranging from 5 – 10 µg/ml are classified as moderately active. On the other hand, compounds with IC<sub>50</sub> values less than 5 µg/ml are considered to be very active. Consequently, the metal complexes under study are considered

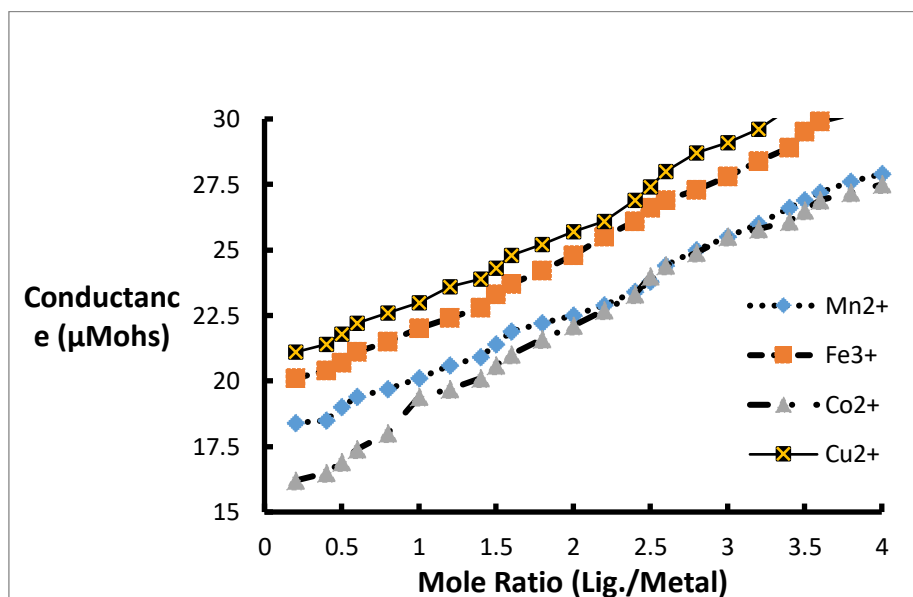
to be of weak activity with IC<sub>50</sub> values ranged from 14 – 27 µg/ml.

### 3- Theoretical studies

#### 3-1 Molecular docking

The antimicrobial activity studies are supported by computational methods such as molecular docking which predicts the preferred orientation of one molecule to a second when bound to each other to form a stable compound [15]. The preferred orientation knowledge may be used to predict the strength of association or binding affinity between the two molecules using, for example, scoring functions. Additionally, the idea behind docking technique is to generate a comprehensive set of conformations of the receptor complex, and then to rank them according to their stability. The antimicrobial experiments of MOE program was carried out to examine the binding mode between the ligand (AF2) and its Mn(II), Fe(III), Co(II), and Cu(II) complexes with i- *Escherichia coli* (*E. coli*) (PDB code: 1HNJ), ii- *Staphylococcus aureus* (PDB code: 2dhn) (*S. aureus*) and iii- *Candida glabrata* (PDB code: 3ro9) (*C. glabrata*). The docking studies showed a feasible interaction between the investigated complexes and the receptor. All the synthesized metal complexes showed well established hydrophobic interactions with the formation of hydrogen bonds and intermolecular bonds. Representative example of the results is shown in Fig. (3) while the results of calculation process, (type of bonds, bond energies, kind of receptors and bond distances), are listed in Table (5). Calculation showed that these complexes exhibit good binding score ranging from -2.5471 to -5.488 Kcal/mol indicating that they may be considered as a good inhibitor.

Table 1

Fig. (1): Conducometric titration of ligands AF4 with,  $MnCl_2$ ,  $FeCl_3$ ,  $CoCl_2$  and  $CuCl_2$ Table (1): Proton – reagent stability constants and stepwise formation constants of  $Mn^{2+}$ ,  $Fe^{3+}$ ,  $Co^{2+}$  and  $Cu^{2+}$  ions with azo compounds AF1 – AF4

Complex	Proton – reagent stability constants	Step – wise formation constants			
		$Mn^{2+}$	$Fe^{3+}$	$Co^{2+}$	$Cu^{2+}$
AF1	$\log K_1^{H^+} = 9.8$	$\log K_f^1 = 4.9$	$\log K_f^1 = 6.6$	$\log K_f^1 = 6.1$	$\log K_f^1 = 6.9$
	$\log K_2^{H^+} = \text{---}$	$\log K_f^2 = \text{---}$	$\log K_f^2 = \text{---}$	$\log K_f^2 = \text{---}$	$\log K_f^2 = \text{---}$
AF2	$\log K_1^{H^+} = 9.3$	$\log K_f^1 = 6.1$	$\log K_f^1 = 7.1$	$\log K_f^1 = 5.3$	$\log K_f^1 = 5.5$
	$\log K_2^{H^+} = 4.9$	$\log K_f^2 = 2.8$	$\log K_f^2 = 3.88$	$\log K_f^2 = 3.3$	$\log K_f^2 = 3.5$
AF3	$\log K_1^{H^+} = 10.6$	$\log K_f^1 = 5.1$	$\log K_f^1 = 4.3$	$\log K_f^1 = 4.8$	$\log K_f^1 = 5.3$
	$\log K_2^{H^+} = 5.8$	$\log K_f^2 = 2.8$	$\log K_f^2 = 3.1$	$\log K_f^2 = 2.7$	$\log K_f^2 = 2.8$
AF4	$\log K_1^{H^+} = 8.2$	$\log K_f^1 = 3.2$	$\log K_f^1 = 4.8$	$\log K_f^1 = 4.2$	$\log K_f^1 = 5.1$
	$\log K_2^{H^+} = \text{---}$	$\log K_f^2 = \text{---}$	$\log K_f^2 = \text{---}$	$\log K_f^2 = \text{---}$	$\log K_f^2 = \text{---}$

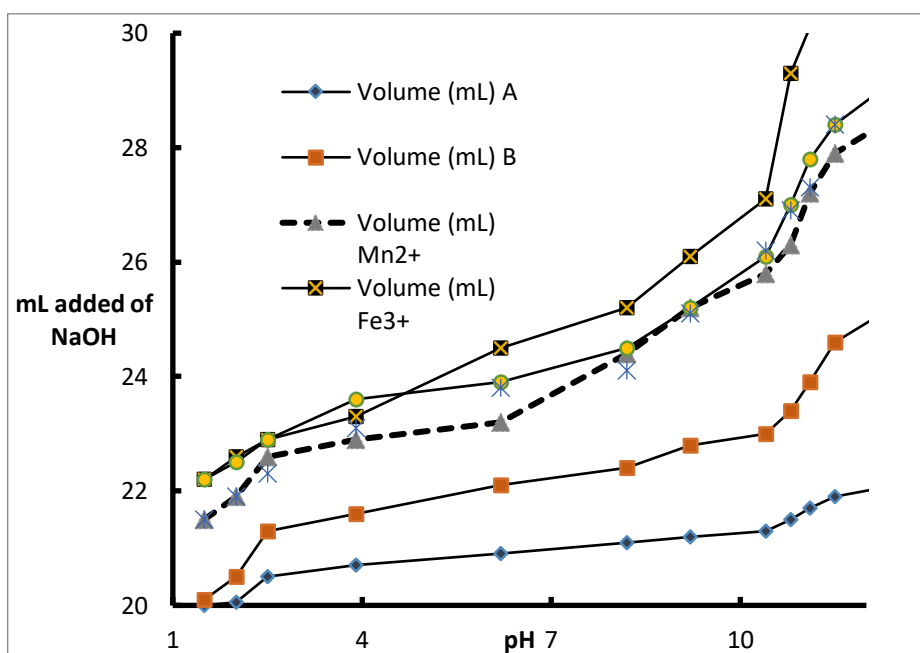


Fig. (2 a): Potentiometric titration of Ligand AF2 in presence of  $Mn^{2+}$ ,  $Fe^{3+}$ ,  $Co^{2+}$  and  $Cu^{2+}$

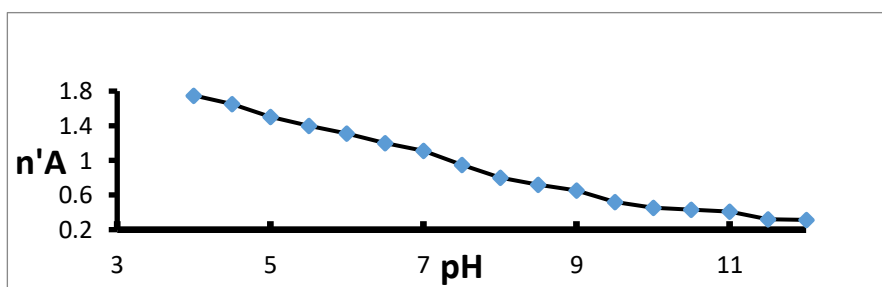


Fig. (2<sub>b</sub>): Formation curve of proton - Ligand AF2

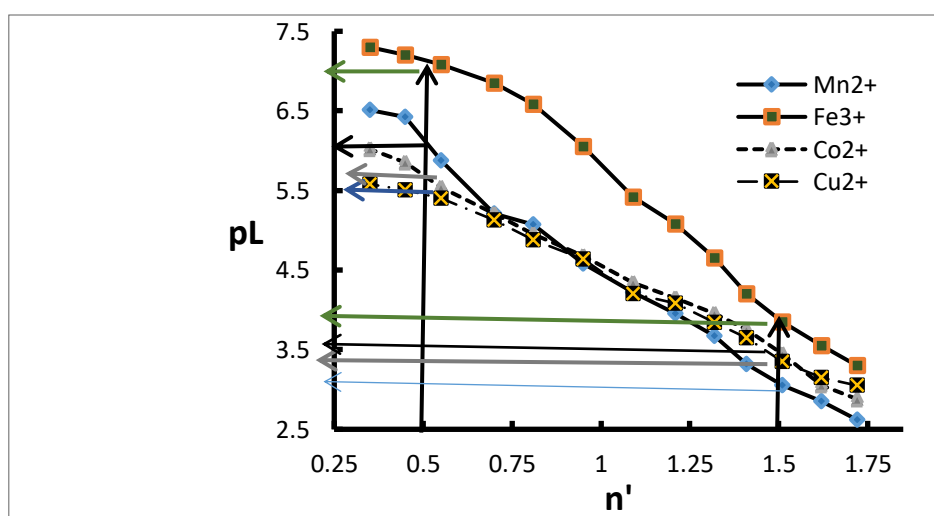


Fig. (2c): Formation curves of Mn<sup>2+</sup>, Fe<sup>3+</sup>, Co<sup>2+</sup> and Cu<sup>2+</sup> complexes with ligand AF2

Table (2): Elemental analysis and molar conductivity of some selected complexes

Complex	Tentative formula	M. Wt.	Elemental analysis				$\Lambda_m^*$
			%C	%H	%N	%M	
AF1-Fe	[C <sub>15</sub> H <sub>10</sub> N <sub>2</sub> O <sub>3</sub> Fe(H <sub>2</sub> O) <sub>3</sub> ] <sup>3+</sup> 3Cl	482.63	37.33	2.07	5.8	11.57	21.12
AF1-Co	[C <sub>15</sub> H <sub>10</sub> N <sub>2</sub> O <sub>3</sub> Co(H <sub>2</sub> O) <sub>3</sub> ] <sup>2+</sup> 2Cl	450.22	39.98	2.22	6.22	13.09	12.22
AF1-Cu	[C <sub>15</sub> H <sub>10</sub> N <sub>2</sub> O <sub>3</sub> Cu(H <sub>2</sub> O) <sub>3</sub> ] <sup>2+</sup> 2Cl	453.83	39.66	2.20	6.17	14	14.47
AF2 Mn	[C <sub>15</sub> H <sub>9</sub> N <sub>2</sub> O <sub>4</sub> Mn(H <sub>2</sub> O) <sub>3</sub> ] <sup>+</sup> Cl	425.52	42.3	2.12	6.58	12.91	12.14
AF2-Co	[C <sub>15</sub> H <sub>9</sub> N <sub>2</sub> O <sub>4</sub> Co(H <sub>2</sub> O) <sub>3</sub> ] <sup>+</sup> Cl	429.02	41.96	2.1	6.53	13.74	33.31
AF3-Fe	C <sub>15</sub> H <sub>10</sub> N <sub>2</sub> O <sub>5</sub> Fe(H <sub>2</sub> O) <sub>3</sub> <sup>3+</sup> 3Cl	514.63	34.98	1.94	5.45	10.85	19.21
AF3-Cu	[C <sub>15</sub> H <sub>10</sub> N <sub>2</sub> O <sub>5</sub> Cu(H <sub>2</sub> O) <sub>3</sub> ] <sup>2+</sup> 2Cl	486.83	36.97	2.05	5.75	13.05	19.88
AF4 Mn	[C <sub>15</sub> H <sub>9</sub> N <sub>2</sub> O <sub>3</sub> ClMn(H <sub>2</sub> O) <sub>3</sub> ] <sup>2+</sup> 2Cl	480.67	37.45	1.87	5.83	11.43	14.33
AF4-Cu	[C <sub>15</sub> H <sub>9</sub> N <sub>2</sub> O <sub>3</sub> ClCu(H <sub>2</sub> O) <sub>3</sub> ] <sup>2+</sup> 2Cl	489.28	36.79	1.84	5.72	12.99	14.55

\* ohm<sup>-1</sup>cm<sup>2</sup>mol<sup>-1</sup>

Table (3): Spectral (in Nojol mull) and magnetic data for some selected complexes.

Complex	wavenumber (cm <sup>-1</sup> )	Assignment	Term symbol	Ground state	Configuration	$\mu_{\text{eff}}$ (BM)
Fe <sup>3+</sup> -AF2	91138.8 22780.6 10161.5	<sup>6</sup> A <sub>1g</sub> (S) → <sup>4</sup> T <sub>1g</sub> (G), → <sup>4</sup> T <sub>2g</sub> (G)a → <sup>4</sup> E <sub>g</sub> ,	<sup>6</sup> S <sub>5/2</sub>	<sup>6</sup> A <sub>1g</sub> (S)	t <sub>2g</sub> <sup>3</sup> e <sub>g</sub> <sup>2</sup>	5.916
Co <sup>2+</sup> - AF2	9115.8 15447.5 18663	<sup>4</sup> T <sub>1g</sub> (F) → <sup>4</sup> T <sub>2g</sub> (F)(v <sub>1</sub> ) → <sup>4</sup> A <sub>2g</sub> (v <sub>2</sub> ), → <sup>4</sup> T <sub>1g</sub> (P)(v <sub>3</sub> )	<sup>4</sup> F <sub>9/2</sub>	<sup>4</sup> T <sub>1g</sub> (F)	t <sub>2g</sub> <sup>5</sup> e <sub>g</sub> <sup>2</sup>	3.783
Cu <sup>2+</sup> - AF3	30303.0 33333.3	<sup>2</sup> a <sub>1g</sub> (D) → <sup>2</sup> b <sub>1g</sub> (D) <sup>2</sup> e <sub>g</sub> (D) → <sup>2</sup> b <sub>1g</sub> (D)	<sup>2</sup> D	<sup>2</sup> E <sub>g</sub>	t <sub>2g</sub> <sup>6</sup> e <sub>g</sub> <sup>3</sup>	1.732

Table (4) Inhibition zone diameter (mm) of some selected metal complexes against various microorganisms

Organism	<i>E. coli</i>			<i>S. aureus</i>			<i>C. glabrata</i>			
	Conc. (μg/mL)	5	10	20	5	10	20	5	10	20
AF1		<b>15</b>	<b>18</b>	<b>25</b>	<b>12</b>	<b>15</b>	<b>25</b>	<b>14</b>	<b>16</b>	<b>22</b>
AF1-Mn(II)		12	17	23	14	20	27	17	19	26
AF1-Fe(III)		17	20	24	12	16	26	16	18	21
AF1-Co(II)		13	18	23	16	20	26	14	18	25
AF1-Cu(II)		18	20	22	16	20	24	14	16	23
<b>AF2</b>		<b>20</b>	<b>24</b>	<b>27</b>	<b>12</b>	<b>17</b>	<b>24</b>	<b>15</b>	<b>18</b>	<b>22</b>
AF2- Mn(II)		16	20	22	16	21	28	20	17	28

---

AF2- Fe(III)	19	24	28	16	18	26	17	20	20
AF2- Co(II)	19	21	25	16	19	26	14	19	24
AF2- Cu(II)	19	23	29	13	19	26	14	19	24

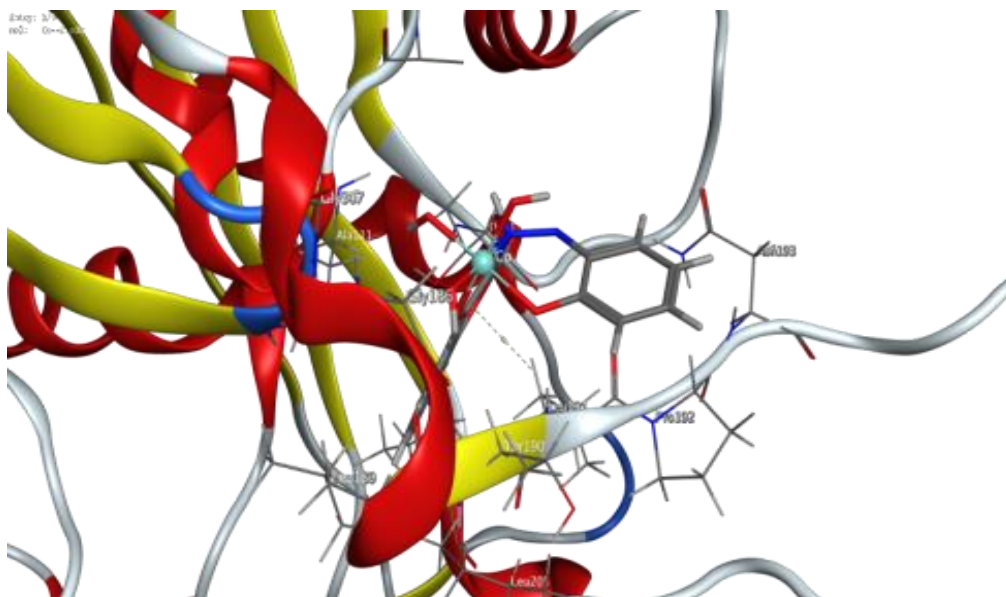
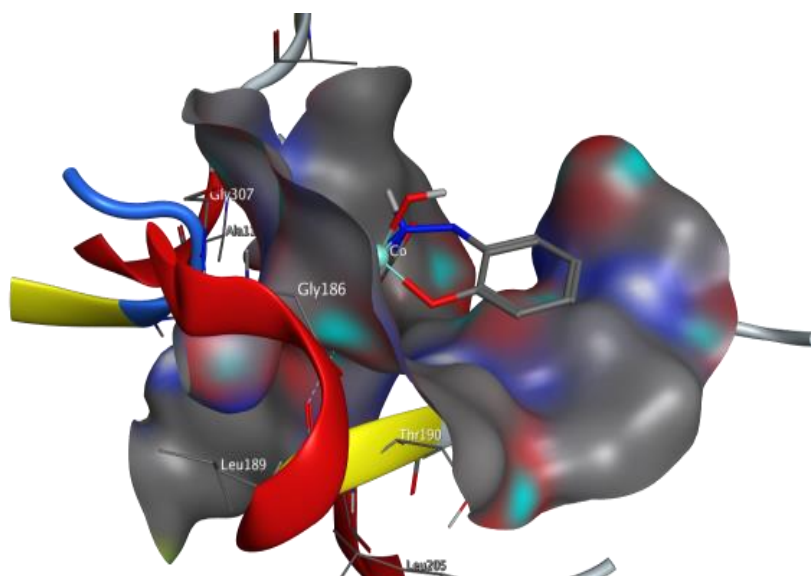
**Fig. (3 - a)****Fig. (3-b)**

Fig. (3 a,b): 3D interaction of the complex AF2-Co complex with the active sites of amino acid residues of protein *Escherichia coli* (PDB code: 1HNJ).

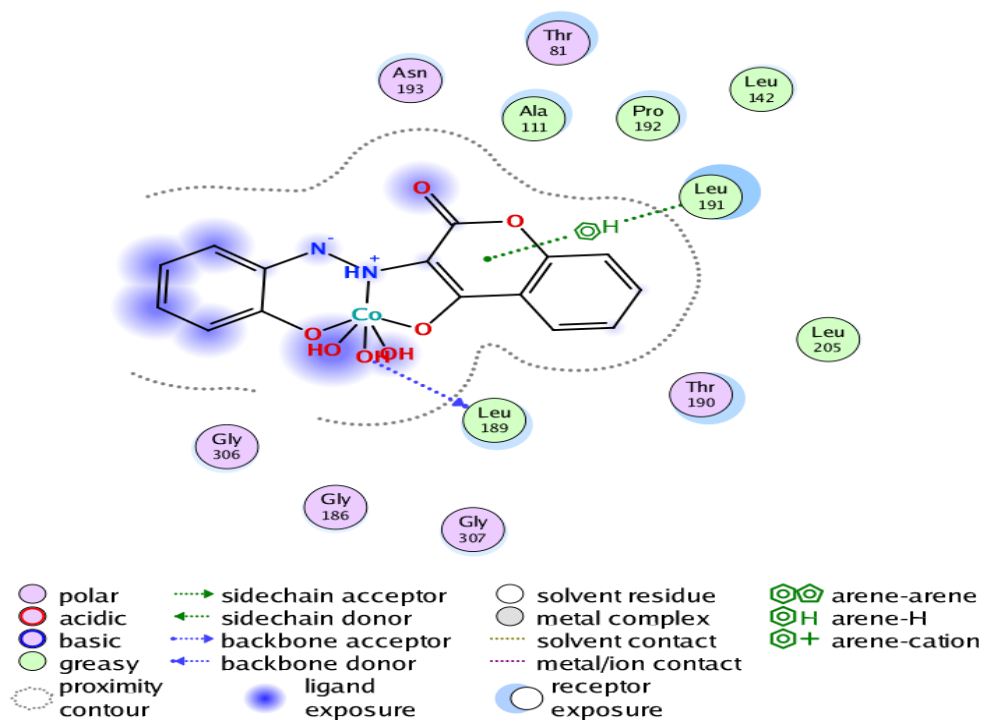


Fig. (3c): 2D interactions of the complex AF2-Co the active site amino acid residues of protein *Escherichia coli* (PDB code: 1HNJ).

Table (5.): The molecular docking data for ligand AF2 and its complexes and *E.coli*, *S. aureus* and *C. glabrata* using MOE 2015.08 software (PDB code: 1HNJ).

Comp.	Organism	Receptor	Bond	Binding energy	Bond length (Å°)	Bond energy
AF2	<i>E.coli</i>	ALA83	H.D	-5.9573	3.28	-0.8
		ASN193	H.A		2.92	-1.0
		THR145	Pi-H		3.72	-0.8
	<i>S. aureus</i>	GLY107	H.D	-2.4721	3.03	-2.4
		PRO109	Pi-H		3.99	-0.9
		PRO106	Pi-H		3.63	-0.8
	<i>C. glabrata</i>	ILE9	H.D	-5.5304	2.88	-0.9
GLY123		H.A	3.36		-1.0	
THR58		Pi-H	4.12		-0.9	
THR58		Pi-H	3.99		-0.7	
<i>E.coli</i>	ASP285	H.D	-4.1209	3.60	-3.5	
	SER10	H.D		2.69	-2.83	
	ASP285	H.D		3.50	-2.97	
AF2-Mn(II)	<i>S. aureus</i>	GLY113	H.A	-3.2180	3.02	-3.0
		THR99	H.A		3.07	-1.3
		GLY113	H.A		3.09	-0.6

AF2- Fe(III)	<i>C. glabrata</i>	MET33	H.D	-5.1977	3.09	-3.8
		LEU25	Pi-H		4.61	-1.0
		LEU25	Pi-H		4.38	-0.6
	<i>E.coli</i>	THR177	H.A	-5.1911	3.06	-1.2
		LYS127	H.A		3.26	-2.1
		LIS178	Pi-H		3.79	-0.8
	<i>S. aureus</i>	GLY111	H.D	-4.7203	2.88	-3.6
		GLY111	H.D		3.19	-3.1
	AF2- Co(II)	<i>C. glabrata</i>	ILE121	H,D	-4.8193	2.71
ALA111			H.A		3.16	-0,7
<i>E.coli</i>		LEU189	H.D	-5.4881	3.17	-1.2
		LEU191	Pi-H		3.70	-0.7
<i>S. aureus</i>		ASN162	H.D	-2.5471	2.89	-3.3
		GLY126	H.D		3.10	-2.0
<i>C. glabrata</i>		GLU32	H.D	-3.0194	3.13	-1,4
		ILE121	H.D		2.88	-2.4
		PHE36	Pi-Pi		3.79	0.00
	PHE36	Pi-Pi		3.79	0.00	
AF2- Cu(II)	<i>E.coli</i>	ASP27	H.D	-5.4881	3.31	-1.3
		TRP32	Pi-Pi		3.49	-0.1
		TRP32	Pi-Pi		3.53	-0.2
	<i>S. aureus</i>	GLU22	H.D	-5.1817	3.41	-0.8
		LYS100	H.A		3.18	-1.3
		ALA18	H.A		3.04	-1.5
	<i>C. glabrata</i>	GLU161	H.D	-4.8574	3.38	-6.9
		GLU161	H.A		2.99	-5.6
		ARG165	H.A		2.93	-2.2
ARG165		H.A		3.2	-3.1	

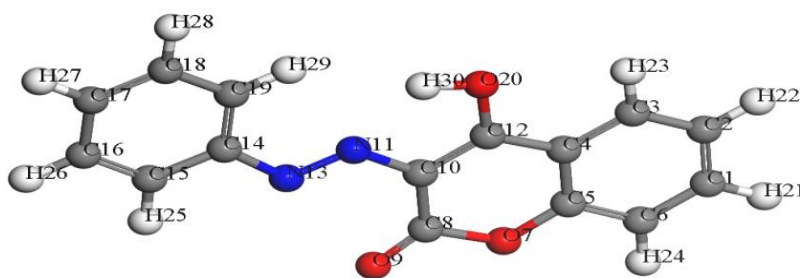


Fig. (4): Molecular modelling of ligand AF1

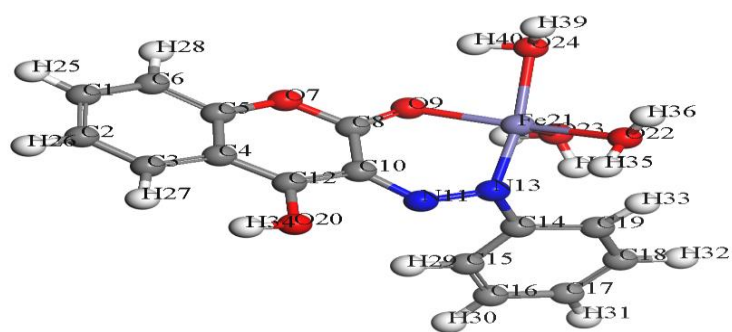


Fig. (5): Molecular modelling of ligand AF1+M<sup>n+</sup> complex

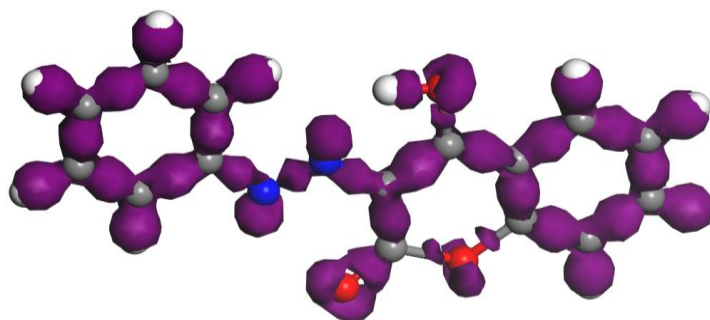


Fig. (6): Deformation density using DFT method for ligand AF1

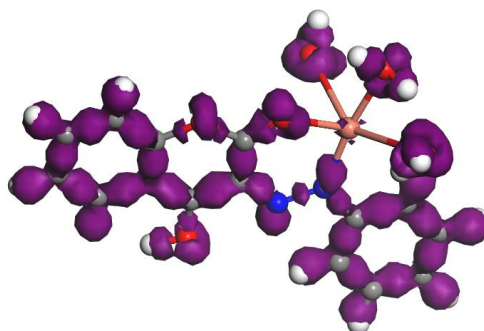


Fig. (7): Deformation density using DFT method for ligand AF1+M<sup>n+</sup> complex

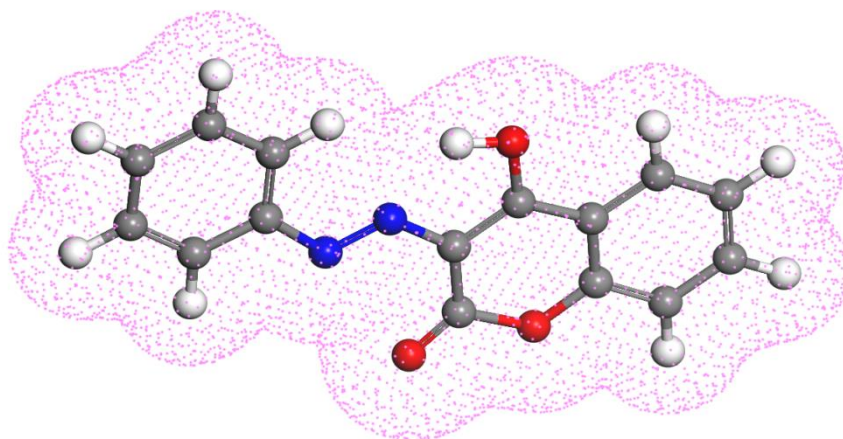


Fig. (8): Total density using DFT method for ligand AF1

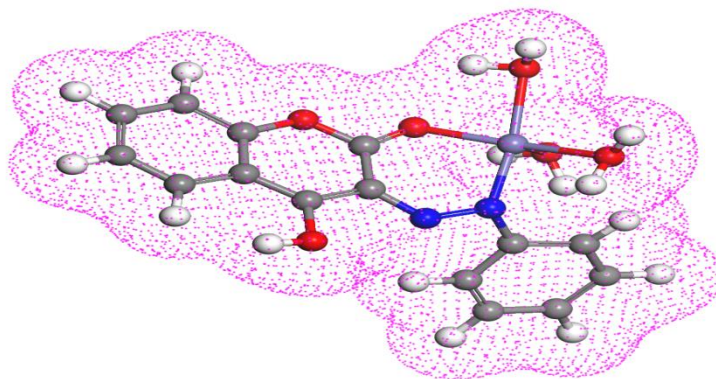
Fig. (9): Total density using DFT method for ligand AF1+Fe<sup>3+</sup>

Table (6): The calculated quantum chemical parameters of ligand AF1 and its complexes

Compound	HOMO	LUMO	$\Delta E$	H	$\Sigma$	X	M	$\Omega$	$\Delta N_{max}$
AF1	-4.944	-3.001	1.943	0.9715	1.029336078	-3.9725	3.9725	8.121850875	4.089037571
AF1-Fe <sup>3+</sup>	-2.602	-2.138	0.464	0.232	4.310344828	-2.37	2.37	12.10538793	10.21551724
AF1-Cu <sup>2+</sup>	-2.927	-2.455	0.472	0.236	4.237288136	-2.691	2.691	15.34212076	11.40254237
AF1-Co <sup>2+</sup>	-3.084	-2.544	0.54	0.27	3.703703704	-2.814	2.814	14.66406667	10.42222222

Table (7): Some energetic properties of ligand AF1 and its complexes calculated by DFT-method

Compound	Energy components (Kcal/mol)						Binding energy (Kcal/mol)
	Sum of atomic energies	Kinetic energy	Electrostatic energy	Exchange-correlation energy	Spin polarization energy	Total energy	
AF1	-19.488 X10 <sup>6</sup>	-6.379X10 <sup>3</sup>	50.649	1.427 X10 <sup>3</sup>	1.207 X10 <sup>3</sup>	-572.97 X10 <sup>3</sup>	-3.695 X10 <sup>3</sup>
AF1-Fe <sup>3+</sup>	-802.42X10 <sup>3</sup>	-3.470X10 <sup>3</sup>	-4.279X10 <sup>3</sup>	1.900X10 <sup>3</sup>	1.419 X10 <sup>3</sup>	-806.86 X10 <sup>3</sup>	-4.431 X10 <sup>3</sup>
AF1-Cu <sup>2+</sup>	-852.20X10 <sup>3</sup>	-5.198X10 <sup>3</sup>	-2.367X10 <sup>3</sup>	1.803X10 <sup>3</sup>	1.357 X10 <sup>3</sup>	-856.61 X10 <sup>3</sup>	-4.406 X10 <sup>3</sup>
AF1-Co <sup>2+</sup>	-817.21X10 <sup>3</sup>	-4.425X10 <sup>3</sup>	-3.336X10 <sup>3</sup>	1.883X10 <sup>3</sup>	1.408 X10 <sup>3</sup>	-821.68 X10 <sup>3</sup>	-4.470 X10 <sup>3</sup>

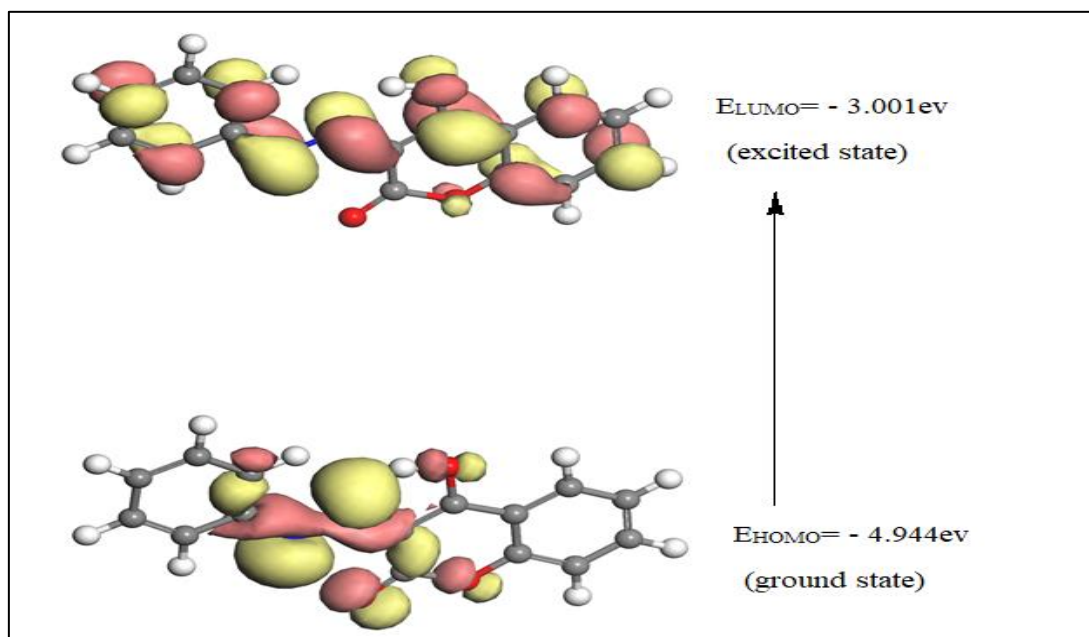


Fig. (10): 3D plots frontier orbital energies using DFT method for ligand AF1

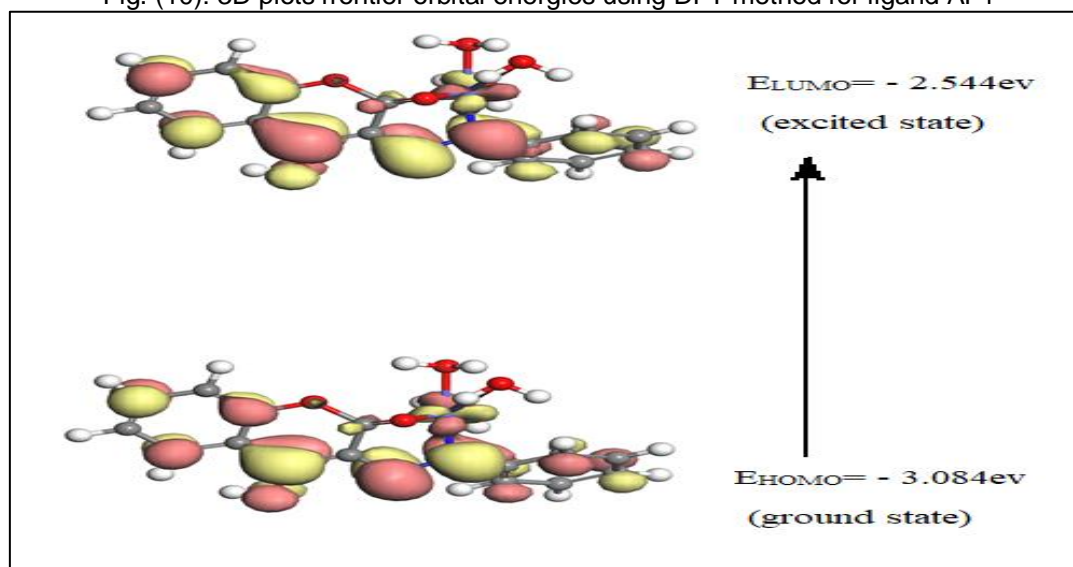
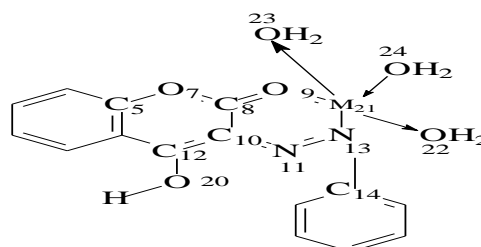


Fig. (11): 3D plots frontier orbital energies using DFT method for the AF1+Co<sup>2+</sup> complex

### 3-2 Molecular modelling

A group of measurements involving DMOL<sup>3</sup> program in materials studio package which is shaped for the wide scale Density Function Theory (DFT) were applied. The Molecular modelling, Total density, Deformation density and 3D plots frontier orbital energies using DFT method for free ligand AF1 and its Fe<sup>3+</sup>, Co<sup>2+</sup> and Cu<sup>2+</sup> complexes were determined and given in Fig.'s (4-11). The molecular modelling of the complexes shows that they can be represented collectively as:



Structure and numeration of the most important atoms of AF1 complexes

**Geometry Optimization:** The geometric parameters (bond lengths and bond angles) of the optimized structures of the AF1 azo ligand

and its complexes were calculated. From the analysis of these data, the following remarks are found:

1- Large variation in N(11)-N(13), N(11)-C(10), O(9)-C(8), and C(10)-C(12) bond lengths of the ligand occurred upon complexation. These bonds show slightly elongation confirming that the coordination took place via azo N(13) atoms and ketonic O(9) groups.

2- All the active groups taking part in coordination have bonds longer than those already existed in the ligands (for example, N=N and C=O). Bond distances become longer due to the formation of the M-O bond which makes the C-O bond weaker

3- New bonds between O(9) – M(21) and N(13) – M(21) are formed in addition to other bonds between M(21) and the oxygen atoms (O) (22, 23 and 24) of the coordinated water molecules

4- Bond angles of the free ligand moiety; O(20) – C(12) – C(10), C(10) – N(11) – N(13) and C(10) – C(8) – O(9) were altered somewhat upon coordination. Also, the bond angles surrounding the central metal atom; O(9) – M(21) – N(13), N(13) – M(21) – O(22), N(13) – M(21) – O(23) and N(13) – M(21) – O(24) in the complexes are quite near to an octahedral geometry predicting  $d^2sp^3$  hybridization [10].

Hence, it is inferred that, coordination of the organic ligand to the metal ions by donating a lone pair of electrons results in a decrease in electron density on the coordinating atoms, and to an increase in the bond lengths and variation in bond angle. Furthermore, in most of the cases, the actual bond angles and lengths are close to the optimal values (most favourable). The 3D optimized geometrical structures of ligand AF1 and its Fe(III), Co(II) and Cu(II) are presented in Fig.,s (4 - 7).

#### Total charge density:

It is the measure of the probability of an electron being present at a specific location and it is usually found around the atom and its bonds. Total density is directly related to chemical reactivity. Red color represents the regions of negative electrostatic potential which is related to electrophilic reactivity. The electron-poor region has blue color (favor site for the nucleophilic attack), while the region with gray color points to the neutral electrostatic potential region. It is found that oxygen and nitrogen atoms of free ligand were surrounded by a greater negative charge surface, making them potentially more favorable for the electrophilic attack. The greater positive charge surrounds the metal ion favoring the complexation process.

Molecular modeling software often provides graphical images of electron charge density by representing the presence of high or low electron density in a particular position of molecules. The total charge density for the ligand AF1 and one of its complexes are shown in Fig.'s (8 and 9)

#### Frontier molecular orbitals

The HOMOs and LUMOs are known as Frontier molecular orbitals (FMOs), which play an important role for evaluating molecular chemical stability, chemical reactivity and hardness-softness of the molecule. Representative picture of Frontier molecular orbitals and Deformation density are shown in Figs. (10 and 11). The HOMO acts as an electron donor, while the LUMO is an electron acceptor. In the HOMO of AF1 molecule, the electron density mainly delocalized over quinolone rings OH and N=N groups. While in the LUMO orbital this density is delocalized on all the three phenyl rings. The energy gap ( $\Delta E$ ) represents the chemical reactivity of compound; lower value of  $\Delta E$  makes the system more reactive or less stable. As depicted in Table 6, the free azo compound AF1 has the largest energy gap which decreases in the following order AF1- Co(II) > AF1- Co(II) > AF1Fe(III). The energy gap  $\Delta E$  is directly involved with hardness/softness of a chemical species. The higher value of  $\Delta E$  represents more hardness or less softness of a compound. Soft molecules are more reactive than hard ones because they could easily offer electrons to an acceptor. Thus the free ligand AF1 referred as hard molecule when compared its metal complexes. Another global reactivity descriptor electrophilicity index ( $\omega$ ) describes the electron accepting ability of the systems quite similar to hardness and chemical potential. High values of electrophilicity index increases electron accepting abilities of the molecules. The electrophilicity index ( $\omega$ ) is positive, definite quantity and the direction of the charge transfer is completely determined by the electronic chemical potential ( $\mu$ ) of the molecule because an electrophile is a chemical species capable of accepting electrons from the environment and its energy must decrease upon accepting electronic charge. Therefore, the electronic chemical potential must be negative exactly as supported by the values in Table (7). The values of ( $E_{\text{HOMO}} - E_{\text{LUMO}}$ ) energies of frontier molecular orbitals, energy band gap that explains the final charge transfer interaction inside the molecule, electronegativity ( $\chi$ ), chemical potential ( $\mu$ ), global hardness ( $\eta$ ), global softness ( $\sigma$ ), additional electronic charge ( $\Delta N_{\text{max}}$ ) and global

electrophilicity index ( $\omega$ ) were calculated and listed in Table (7):

$$\chi = -1/2 (E_{\text{LUMO}} + E_{\text{HOMO}}) \quad \mu = -\chi = 1/2 (E_{\text{LUMO}} + E_{\text{HOMO}}) \quad \eta = 1/2 (E_{\text{LUMO}} - E_{\text{HOMO}})$$

$\Delta N_{\text{max}} = -\mu / \eta$ ,  $\omega = \mu^2 / 2 \eta$ , The inverse value of the global hardness is designed as the softness ( $\sigma$ );  $\sigma = 1 / \eta$ .

### Conclusion

A series of azo compounds based on 4-hydroxycoumarin along with their metal complexes with Mn(II), Fe(II), Co(II), and Cu(II) metal ions were prepared and characterized by different techniques. The stoichiometry of metal complexes formed in solution, studied by conductometric titrations, showed the probable formation of 1:1, 1:2 and 2:1 (M:L) complex species. The proton – reagent stability constants of the free ligands and the metal – ligand stability constants of the complexes formed in solution were determined by potentiometric technique. From the molar conductivity and spectral data it was concluded that the ligands behaved as monobasic bidentate ligand with NO coordination fashion leading to the formation of octahedral geometries for all complexes. The antimicrobial studies against *Escherichia coli*, *Staphylococcus aureus* and *Candida glabrata* (*C. glabrata*) showed that the selected studied compounds exhibit high activity against the tested organisms compared to levofloxacin taken as a standard drug. The antimicrobial activity studies were supported by computational methods such as molecular docking. The docking studies had been applied to explore the binding interaction of ligand Afs and its complexes with active site of DNA. The cytotoxic activities of some selected metal complexes were tested against HEPG2 cell line and compared to that of Vinblastine as a standard drug. The metal complexes under study are considered to be of weak activity with IC<sub>50</sub> values ranged from 14 – 27  $\mu\text{g/ml}$ . A group of measurements involving DMOL<sup>3</sup> program in materials studio package with Density Function Theory (DFT) were applied for the compound AF1 and its complexes. From this study, the binding energies, bond length and dipole moment were calculated.

### References

- [1] M. Ayaz, F. Ali, G. Shabir, A. Saeed, N. Ali, N. Abbas, G. Hussain and P. A. Channar, "New acid dyes and their metal complexes: dyeing, thermal and antifungal behaviour, J. appl. res. technol 17(1), (2019).
- [2] S. M H obaida, A. E. Abd-Almonuimb, A. J. Jarada, " Synthesis, Characterization, Industrial And

Biological Application Of Co(II), Ni(II), Cu(II) And Zn(II) Complexes With Azo Ligand Derived From Metoclopramide Hydrochloride And 3,5-Dimethylphenol", Egypt. J. Chem. , 63, (12), (2020), 4719 – 4729.

- [3] J. M. Mahmood Al-Zinke and A. J. Jarad, "Synthesis, Spectral Studies and Microbial Evaluation of Azo Dye Ligand Complexes with Some Transition Metals", J. Pharm. Sci. & Res. 11(1), (2019), 98-103
- [4] S. Prakash, G. Somiya, N. Elavarasan, K. Subashini, S. Kanaga, R. Dhandapani, M. Sivanandam and P. Kumaradhas, " Synthesis and characterization of novel bioactive azo compounds fused with benzothiazole and their versatile biological applications", J. Molec. Struc., 1224, (15), (2021), 129016
- [5] Y. Ali, S. Abd Hamid and U. Rashid, " Biomedical Applications of Aromatic Azo Compounds", Mini-Reviews in Medicinal Chemistry, 18 , (18) , 2018 DOI : [10.2174/1389557518666180524113111](https://doi.org/10.2174/1389557518666180524113111)
- [6] W. H. Mahmoud, M. M. Omar and Fatma N. Sayed, " Synthesis, spectral characterization, thermal, anticancer and antimicrobial studies of bidentate azo dye metal complexes J. Thermal Analysis & Calor. 124, (2016), 1071–1089.
- [7] Swati , M. Gupta, R. Karnawat, I.K. Sharma and PS Verma, " Biological and Chemical Sciences Synthesis, Spectroscopic Characterization and Antibacterial Activity of 2-[2- Hydroxyphenylazo]-1-naphthol-4-sulphonic acid and its Fe (III) Co (II) and Cu (II) complexes", Res. J. Pharm., 4, (1), (2011), 805-811
- [8] A. A. Allothman, M. D. Albaqami and A. R. Alshgari, " Synthesis, spectral characterization, quantum chemical calculations, thermal studies and biological screening of nitrogen and oxygen donor atoms containing Azo-dye Cu(II), Ni(II) and Co(II) complexes", J. Molec. Struc., 1223 (5), ( 2021), 128984
- [9] K. S. Abou Melha, G. A. Al-Hazmi, I. Althagafi, A. Alharbi, A. A. Keshk, F. Shaaban, N. El-Metwaly, "Spectral, Molecular Modeling, and Biological Activity Studies on New Schiff's Base of Acenaphthaquinone Transition Metal Complexes", *Bioinorganic Chemistry and Applications*, 2021, Article ID 6674394, 17 pages, 2021. <https://doi.org/10.1155/2021/6674394>.

- [10] G. G. Mohamed, W. H. Mahmoud, and A. M. Refaat, "Nano-Azo Ligand and Its Superhydrophobic Complexes: Synthesis, Characterization, DFT, Contact Angle, Molecular Docking, and Antimicrobial Studies", *J. Chem.*, 2020, Article ID 6382037, 19 pages, 2020. <https://doi.org/10.1155/2020/6382037>
- [11] Islam M.I. Moustafa and Magda H. Abdellatif, "Synthesis, Spectroscopic Studies and Biological Evaluation of Co(II), Ni(II), Cu(II) and Zr(IV) Complexes of Azo Dyes and Thiamine Hydrochloride as Antimicrobial Agents", *Mod. Chem. Appl.*, 5, (1), (2017), 1-7. DOI: 10.4172/2329-6798.1000202
- [12] Yu. H. Kazuki and K. Sigeo "ESR spectra of the square planar copper(II) complexes with various N<sub>4</sub>-macrocyclic ligands" *J. Coordination Chem.*, 10(1-2), (1980), 101-105.
- [13] D. B. Vivekanand and B. H. Mruthyunjayaswamy "Synthesis Characterization and Antimicrobial Activity Studies of Some Transition Metal Complexes Derived from 3-Chloro-N'-[(1E)-(2-hydroxyphenyl)methylene]-6-methoxy-1-benzothioephene-2 carbonylhydrazide", *ScientificWorldJournal*, Published online 2013 Dec 26. doi: [10.1155/2013/451629](https://doi.org/10.1155/2013/451629)
- [14] C. Jayabalakrishnan and K. Natarajan "Synthesis, characterization and biological activity of ruthenium(II) carbonyl complexes containing bifunctional tridentate Schiff bases" *Trans Met Chem.*, (2001), 26: 105-109.
- [15] S. Mondal, S. M. Mandal, T. Kumar Mondal and C. Sinha; "Spectroscopic characterization, antimicrobial activity, DFT computation and docking studies of sulfonamide Schiff bases" *J. Mole. Struc.* 1127, (5) (2017), 557-567
- [16] B. Delley, *Phys. Rev. B: Condens. Matter*, 66(2002), 155-125.
- [17] in: *Materials Studio*, Accelrys software Inc. San Diego, USA, (2011).
- [18] W. J. Hehre, *Ab initio molecular orbital theory*, Wiley-Interscience, (1986).
- [19] Mostafa M. E., *Physicochemical studies of some multidentate azo dye and their chelates with transition metal ions*, Ph.D. thesis, Faculty of Science, Benha University (1988) b47-51.
- [20] J. Bjerrum; "Metal amine formation in aqueous solution", P. Haas & Son, Copenhagen, p.20 (1941).
- [21] A. Earnshaw; *Introduction to Magnetochemistry*, Academic Press Inc Limited, London, 34, (1968).
- [22] M. B. Halli, Ravindra. S. Malipatil, *Der Pharma Chemica.*, 3, (2011), 146.
- [23] U. G. Pranita, P. R. Mandlik and A. S. Aswar "Synthesis and Characterization of Cr(III), Mn(III), Fe(III), VO(IV), Zr(IV) and UO<sub>2</sub>(VI) Complexes of Schiff Base Derived from Isonicotinoyl Hydrazone" *Ind. J. Pharm. Sci.*, 77(4), (2015) : 376-381
- [24] J. G. Malecki, M. Bałanda, Groń, T. *et al.* Molecular, spectroscopic, and magnetic properties of cobalt(II) complexes with heteroaromatic N(O)-donor ligands. *Struct Chem* 23, 1219–1232 (2012).
- [25] P. Kopel, Z. Travnicek, L. Kvitek, M. Biler, M. Paylicek, Z. Sindelar and J. Marek "Trithiocyanurate complexes of iron, manganese and nickel and their anticholinesterase activity" *Trans. Met. Chem.*, 26(3), (2001), 282 – 286.
- [26] S. A. Shaker, Y. Farina, S. Mahmoud and M. Eskender "Co(II), Ni(II), Cu(II) and Zn(II) mixed ligand complexes of 6-aminopurine, theophylline and thiocyanate ion, preparation and spectroscopic characterization" *ARPN J. Eng. Appl. Sci.*, (2009), 4(9).
- [27] G. G. Mohamed, M. M. Omar, M. S. A. El-Ela, and A. M. M. Hindy, "Preparation of macrocyclic Schiff-base ligand and antibacterial activities of transition metal complexes thereof," *Toxic. Environ. Chem.*, (2011), 93, (1), 57–72,
- [28] N. Raman, R. Jeyamurugan, M. Subbulakshmi, R. Boominathan, and C. R. Yuvarajan, "Synthesis, DNA binding, and antimicrobial studies of novel metal complexes containing a pyrazolone derivative Schiff base," *Chemical Papers*, 64, (3), (2010), 318–328, 2010.
- [29] N. Dharmaraj, P. Viswanathamurthi, and K. Natarajan, "Ruthenium(II) complexes containing bidentate Schiff bases and their antifungal activity," *Trans. Metal Chem.*, 26, (1-2), (2001), 105–109.
- [30] Z. H. Chohan, M. Arif, M. A. Akhtar, and C. T. Supuran, "Metal-based antibacterial and antifungal agents: synthesis, characterization, and in vitro biological evaluation of Co(II), Cu(II), Ni(II), and Zn(II) complexes with amino acid-derived compounds," *Bioinorg. Chem. Appl.*, 2006, Article ID 83131, 13 pages, 2006.
- [31] W. T. Shier; *Mammalian Cell Culture on \$ 5 a day: a Laboratory Manual of Low Cost Methods*. University of the Philippines, Los Banos, (1991).